L/E analysis of the atmospheric neutrino data from Super-Kamiokande

I.HIGUCHI[1] ET AL. FOR THE SUPER-KAMIOKANDE COLLABORATION
[1]*Institute for Cosmic Ray Research, University of Tokyo 5-1-5 Kashiwanoha, Kashiwa 277-8583, Japan*
higuchi@icrr.u-tokyo.ac.jp

Abstract: Muon neutrino disappearance probability as a function of neutrino flight length L over neutrino energy E was studied. A dip in the L/E distribution was observed in the data from both Super-Kamiokande-I and -II, as predicted from the sinusoidal flavor transition probability of neutrino oscillation. The observed L/E distribution constrained $\nu_\mu \leftrightarrow \nu_\tau$ neutrino oscillation parameters. In addition, data are used to constrain the decay and decoherence parameters.

Introduction

Super-Kamiokande is a 50,00 ton water Cherenkov detector located 1,000 m (2,700 m water equivalent) under Mt. Ikenoyama at Kamioka Observatory, Gifu Prefecture, Japan. The detector is a cylindrical tank and is optically divided into two regions. The inner detector (ID) is instrumented with 11,146 for Super-Kamiokande-I and 5,182 for Super-Kamokande-II inward facing 20 inch PMTs which give a photo cathode coverage of 40 % for Super-Kamokande-I and 19 % for Super-Kamiokande-II. The outer detector (OD) completely surrounds the ID with the thickness of 2.05 m to 2.2 m water and is monitored by 1,885 outward-facing 8 inch PMTs. The OD works as a veto counter against cosmic ray muons. The charge information observed in the OD is also used in the L/E analysis.

L/E analysis

Atmospheric neutrino was observed in Super-Kamiokande-I and Super-Kamiokande-II during 1489 and 803 live-days exposure, respectively. The atmospheric neutrino events are classified into fully contained (FC) and partially contained (PC) respectively. The vertices of neutrino interactions are required to be inside the fiducial volume of the ID for these events. If the tracks of entire particles are contained inside the ID, the event is classified as FC. If one of the particles, mostly a muon, exits the ID and deposits visible energy in the OD, the event is classified as PC. Each observed Cherenkov ring is identified as either e-like or μ-like based on the ring pattern. The directions and the momentum of charged particles can be reconstructed from the ring image. The atmospheric neutrino events in Super-Kamiokande are predicted by a detailed Monte Carlo simulation [2].

In the L/E analysis, PC events is subdivided into two categories :'OD stopping events' where the muon stops in the outer detector, and 'OD through-going events' where the muon exit into the rock. This division is based on the amount of Cherenkov light detected in the OD. Since these two samples have different resolution in L/E, different cuts were applied for each sample, improving the overall efficiency.

The neutrino energy is estimated from the total energy of charged particles observed in the ID. The energy deposited in the OD is estimated from the potential track length in the OD and is taken into account for PC events. The relationship between the neutrino energy and the observed energy is determined based on the Monte Carlo simulation. The flight length of neutrinos, which ranges from approximately 15 km to 13,000 km depending on the zenith angle, is estimated from the direction of the total momentum of the observed particles.

The resolution of the reconstructed L/E is calculated at each point of the ($\cos\theta$,E_ν) plane, where θ

is the zenith angle. The L/E resolution cut is set to be $\Delta L/E < 70\%$ from the Monte Carlo simulation to maximize the sensitivities to distinguish neutrino oscillation from other hypotheses.

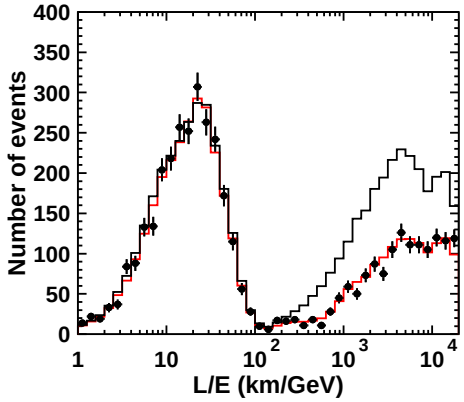

Figure 1: Number of events as a function of the reconstructed L/E for the data (point), the atmospheric neutrino Monte Carlo events without neutrino oscillation(histogram) and the best-fit expectation for 2-flavor $\nu_\mu \leftrightarrow \nu_\tau$ oscillations (red line) from Super-Kamiokande-I+II.

A fit to the observed L/E distributions was carried out assuming neutrino oscillations. In the analysis, the L/E distribution is divided into 43 bins between $log(L/E) = 0.0$ and 4.3 for Super-Kamiokande-I and Super-Kamiokande-II separately. The likelihood of the fit and the χ^2 are defined as :

$$\mathcal{L}(N^{\rm prd}, N^{\rm obs}) = \prod_{i=1}^{86} \frac{\exp(-N_i^{\rm prd})(N_i^{\rm prd})^{N_i^{\rm obs}}}{N_i^{\rm obs}!} \times \prod_{j=1}^{42} \exp\left(-\frac{\epsilon_j^2}{2\sigma_j^2}\right)$$

$$\chi^2 \equiv -2\ln\left(\frac{\mathcal{L}(N^{\rm prd}, N^{\rm obs})}{\mathcal{L}(N^{\rm obs}, N^{\rm obs})}\right)$$

where $N_i^{\rm obs}$ is the number of the observed events in the i-th bin and $N_i^{\rm prd}$ is the number of predicted events, in which neutrino oscillation and systematic uncertainties are considered. 42 systematic uncertainties are considered in the L/E analysis, which include uncertainty parameters from the neutrino flux calculation, neutrino interaction

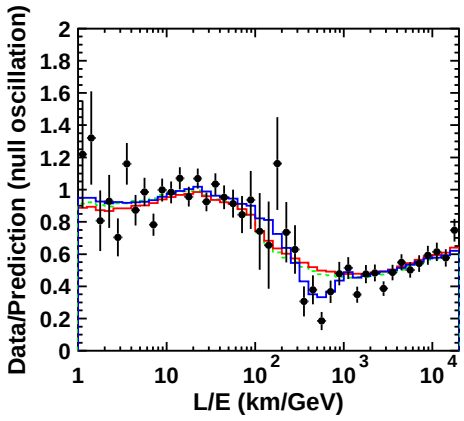

Figure 2: Ratio of the data to the non-oscillated Monte Carlo events (points) with the best-fit expectation for 2-flavor $\nu_\mu \leftrightarrow \nu_\tau$ oscillations (blue line). Also shown are the best-fit expectation for neutrino decay (red line) and neutrino decoherence (green line) from Super-Kamiokande-I+II.

models and detector performance. Among these, only 32 constrain the likelihood as the absolute normalization is allowed to be free. The second term in the likelihood definition represents the contributions from the systematic errors, where σ_j is the estimated uncertainty in the parameter ϵ_j. A scan was carried out on a $(\sin^2 2\theta, \log \Delta m^2)$ grid, minimizing χ^2 by optimizing the systematic error parameters at each grid point.

The minimum χ^2 is 83.9/83 d.o.f at $(\sin^2 2\theta, \Delta m^2) = (1.00, 2.3 \times 10^{-3} eV^2)$, where θ is the mixing angle and $\Delta m^2 = m_3^2 - m_2^2$ is the difference of the squared mass of ν_3 and ν_2. Including unphysical parameter region $(\sin\theta^2 > 1)$, the best-fit is obtained at $(\sin^2 2\theta, \Delta m^2) = (1.03, 2.4 \times 10^{-3} eV^2)$

Figure 1 shows the number of events as a function of L/E for the data and Monte Carlo predictions without oscillation, Figure 2 shows the data over non-oscillated Monte Carlo ratio with the best-fit expectation for 2-flavor $\nu_\mu \leftrightarrow \nu_\tau$ oscillations in which systematic errors are considered. A dip, which should correspond to the first oscillation minimum, was observed around $L/E = 500\, km/GeV$ for Super-Kamiokande-I+II data. The observed L/E distribution, especially the first dip, gives the direct evidence that the neu-

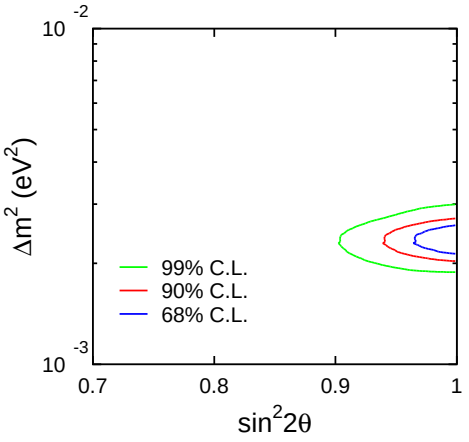

Figure 3: 68,90 and 99 % C.L. allowed oscillation parameter regions for 2-flavor $\nu_\mu \leftrightarrow \nu_\tau$ oscillations obtained by the L/E analysis from Super-Kamiokande-I+II.

trino flavor transition probability obeys the sinusoidal function as predicted by neutrino flavor oscillations. Figure 3 shows the contour plot of the 68, 90 and 99 % C.L. allowed oscillation parameter regions for the Super-Kamiokande-I and -II data.

Constraints on exotic models

The observed L/E distribution was also fitted by assuming neutrino decay[4, 3] and neutrino decoherence[5] assumptions. Figure 2 includes the best-fit expectation for neutrino decay and decoherence.

A fit to the data is carried out assuming that neutrino oscillation and neutrino decay (or decoherence) coexist. In each case, the neutrino flavor transition can be expressed by 3 parameters; $(\cos^2\theta, m_2/\tau_2, \Delta m^2)$ for neutrino oscillation plus neutrino decay and $(\sin^2 2\theta, \gamma_0, \Delta m^2)$ for neutrino oscillation plus neutrino decoherence. The definition of the log likelihood and the systematic errors used in the fit are identical to that for the neutrino oscillation analysis. Figure 4 and 5 show the contour plots of the allowed parameters region projected to the $(m_2/\tau_2, \Delta m^2)$ and $(\gamma_0, \Delta m^2)$ plane marginalizing the mixing angle parameters θ. The minimum value of the χ^2 is 83.8/83 d.o.f. obtained at $(\cos^2\theta, m_2/\tau_2, \Delta m^2) = (0.5, 0\ GeV/km, 2.4 \times 10^{-3} eV^2)$ for neutrino decay plus neutrino oscillation and the χ^2 is 83.8/83 d.o.f. obtained at $(\sin^2 2\theta, \gamma_0, \Delta m^2) = (1.0, 0.0\ GeV, 2.4 \times 10^{-3} eV^2)$ for neutrino decoherence plus neutrino oscillation. Three contours correspond to the 68, 90 and 99 % C.L. allowed regions. In both scenario, pure neutrino oscillation was most favored.

In the case of neutrino oscillation plus decay scenario, the decay parameter is constrained to $m/\tau < 3.2 \times 10^{-5} GeV/km$ at 90% C.L. The limit on the decay parameter is improved compared with the previous work [4]. There is a small allowed region at 99 % around $m/\tau \sim 10^{-3} GeV/km$. $m/\tau \sim 1.6 \times 10^{-2} GeV/km$ together with $(\Delta m^2 = 0)$ was the original suggestion in [4]. We have already excluded the pure neutrino decay model[2]. Compared with the originally suggested m/τ value [3], the present 90 % C.L. limit is smaller by nearly 3 orders of magnitude. No evidence for finite decay component was observed.

In the case of neutrino oscillation plus decoherence scenario, the decoherence parameter is constrained to $\gamma_0 < 1.4 \times 10^{-22} eV^2$ at 90% C.L. The limit on the decoherence parameter is improved by one order of magitude compared with the previous work [5]. We have already exclude the pure neutrino decoherence model. Our current analysis even disfavors the oscillation plus decoherence hybrid model with $\gamma_0 \sim 10^{-22} eV^2$ at 90% C.L. No evidence for finite decoherence component was observed.

Conclusions

L/E analysis were carried out using atmospheric neutrino data from Super-Kamiokande-I+II. A dip in the L/E distribution was observed, as predicted from the sinusoidal flavor transition probability of neutrino oscillation. The allowed neutrino oscillation parameter region, especially the Δm^2 regions, was tightly constrained. Furthermore, the parameters for the decay or the decoherence model are constrained based on the oscillation plus decay or the oscillation plus decoherence hybrid models. No evidence for the sub-leading decay or decoherence effect was observed.

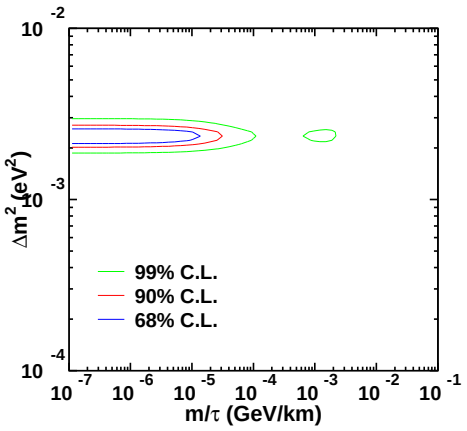

Figure 4: Contour plot of the allowed parameter regions projected to the $(m_2/\tau_2, \Delta m^2)$ plane optimizing the mixing angle parameter $\cos^2\theta$. The horizontal axis shows m_2/τ_2 which characterizes neutrino decay and vertical axis shows Δm^2 which characterizes neutrino oscillation. The small Δm^2 region corresponds to the neutrino decay dominant case.

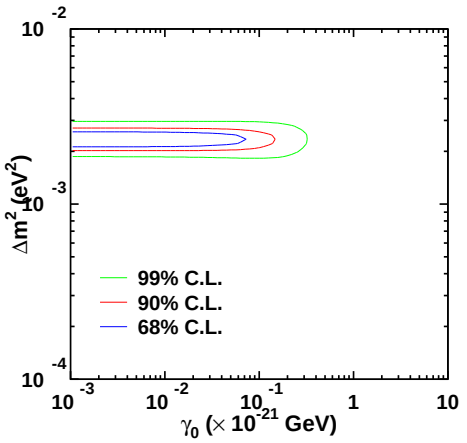

Figure 5: Contour plots of the allowed parameters regions projected to the $(\gamma_0, \Delta m^2)$ plane optimizing the mixing angle parameters $\sin^2\theta$. The horizontal axis shows γ_0 which characterizes neutrino decoherece and vertical axis shows Δm^2 characterizes neutrino oscillation. The small Δm^2 region corresponds to the neutrino decoherence dominant case.

References

[1] Y. Ashie et al. Evidence for an oscillatory signature in atmospheric neutrino oscillation. *Phys. Rev. Lett.*, 93:101801, 2004.

[2] Y. Ashie et al. A measurement of atmospheric neutrino oscillation parameters by super-kamiokande i. *Phys. Rev.*, D71:112005, 2005.

[3] Vernon D. Barger et al. Neutrino decay and atmospheric neutrinos. *Phys. Lett.*, B462:109–114, 1999.

[4] Vernon D. Barger, J. G. Learned, S. Pakvasa, and Thomas J. Weiler. Neutrino decay as an explanation of atmospheric neutrino observations. *Phys. Rev. Lett.*, 82:2640–2643, 1999.

[5] E. Lisi, A. Marrone, and D. Montanino. Probing possible decoherence effects in atmospheric neutrino oscillations. *Phys. Rev. Lett.*, 85:1166–1169, 2000.